PCCP

Accepted Manuscript




ROYAL SOCIETY OF CHEMISTRY

www.rsc.org/pccp

Cite this: DOI: 10.1039/c0xx00000x

www.rsc.org/xxxxxx

ARTICLE TYPE

# Intermolecular X…X (X = C, N and O) Dipole Interaction between Atoms in Similar Chemical Environment

**Karunakaran Remya and Cherumuttathu H. Suresh***

***Received (in XXX, XXX) Xth XXXXXXXXX 20XX, Accepted Xth XXXXXXXXX 20XX***

**DOI: 10.1039/b000000x**

Clear evidence for intermolecular carbon-carbon (Cé C), nitrogen-nitrogen (Né N) and oxygen-oxygen (Oé O) interactions between atoms in similar chemical environment in homogeneous dimers of organic molecules are obtained from molecular orbital (MO), natural bond orbital (NBO) and atoms-in-molecule (AIM) electron density analyses at M06L/6-311++G(d,p) level of DFT. These Xé X type interactions are mainly due to local polarization effects, causing segregation of electron rich and electron deficient regions in X atoms, leading to complementary electrostatic interactions between them. NBO analysis provides evidence for charge transfer between the two X atoms. Even for symmetrical molecules such as acetylene, induced dipoles in the dimer creates Cé C bonding interaction. The strength of this type of interaction increases with increase in the dipole moment of the molecule. The energy decomposition analysis (EDA) shows that electrostatic component of the interaction energy ($E_{int}$) is very high (up to 95.86%). Cé C interaction between similar carbon atoms are located in several crystal structures reported in the literature. Further, the MO, AIM and electrostatic potential analysis support Oé O and Né N interaction between similar atoms in many molecular dimers. A good prediction of $E_{int}$ is achieved in terms of total gain in electron density at the non-covalently interacting intermolecular bonds (×ʆ) and monomer dipole moment (µ). A rigorously tested QSAR equation is derived to predict $E_{int}$ for all dimer systems ($E_{int}$ (kcal/mol) = -138.395×ʆ (au) ï 0.551µ (Debye)). This equation suggests that polarization induced bonding interaction between atoms in similar chemical environment could be a general phenomenon in chemistry. The results are further validated using different density functionals and G3MP2 method.

Dedicated to Professor Shridhar R. Gadre on the occasion of his 65th birthday.

## Introduction

Development of new theoretical as well as experimental techniques has led to better understanding of non-covalent interactions. This led to the discovery of several new types of inter molecular interactions involving halogens[1-8], chalcogens[9-14] and pnicogens.[15-16] Non covalent interactions involving group IV elements have recently gained interest[17-28]. The non covalent interaction of a covalently bonded group IV element with an electron donor site has been grouped as a ů hole[4, 29] bonding interaction along with halogen, chalcogen and pnicogen bonds by Politzer *et al*[8, 30-32]. After that, a detailed study on the interaction of ů hole of $F_3MX$ (M = C, Si, Ge and X = F, Cl, Br, I) with the lone pair on nitrogen of HCN is published by Bundhun *et al*[18]. The term ócarbon bondô for the interaction of electron deficient carbon with electron rich centers of molecules like $H_2O$ and $H_2S$ is introduced by Arunan and Mani[19]. They predicted the ócarbon bondô to be important in hydrophobic interactions as well as in the stabilization of intermediate of $S_N2$ reaction. Bauzá *et al*[17] coined the term ótetrel bondingô for describing the interaction of heavier group IV elements with nucleophilic centres. The concept of ódicarbon bondô (similar to dihydrogen bond) between a donor and an acceptor carbon atom in complexes of CO with $CH_3$-X is described by Varadwaj *et al*[28].

A previous study by us on the cooperative clustering of acetonitrile[33] showed that the patterns with maximum number of antiparallel orientations own maximum stability and cooperativity. The atoms-in-molecules (AIM) analysis showed bond critical points (BCPs) and bond paths between the nitrile carbon atoms of two acetonitrile molecules with antiparallel orientations along with hydrogen bonding interactions. These intermolecular Cé C interactions were unusual, since they were observed between carbon atoms of similar chemical environment. The studies reported in literature so far deal with donor-acceptor type interactions where donor and acceptor atoms belong to different chemical environments. This led us to the search for intermolecular interaction between atoms in similar chemical environments in molecules with different functional groups.

In this paper, dimers of several organic molecules with different functionalities, rich in multiple bonds, and most of them with an inherent dipole moment are studied for intermolecular Cé C interaction between carbon atoms in similar chemical environment. Evidence for such Cé C interactions is shown

using AIM and molecular orbital (MO) analyses. Strong evidence for such interactions is given in crystal structures of several organic compounds from literature. We have also shown intermolecular Né N and Oé O interactions between nitrogen

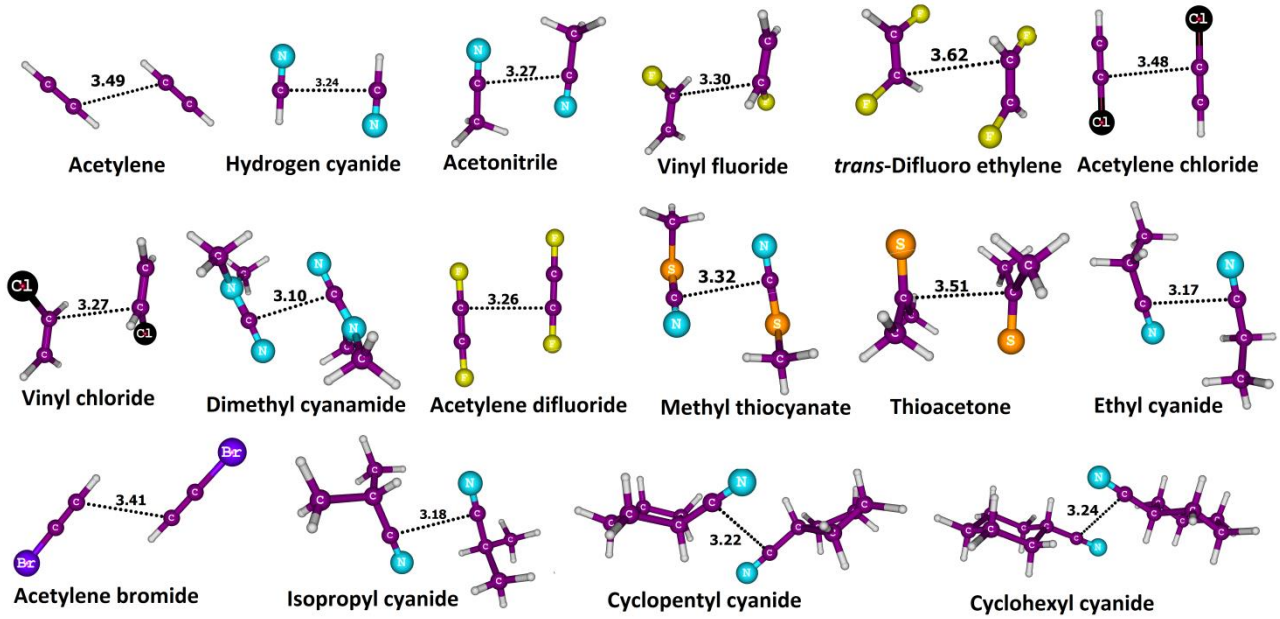


**Figure 1.** Dimers showing Cé C interactions (dotted lines) between carbon atoms in similar chemical environment. Distances are given in Å. Interactions other than Cé C type are not marked in the figure for simplicity

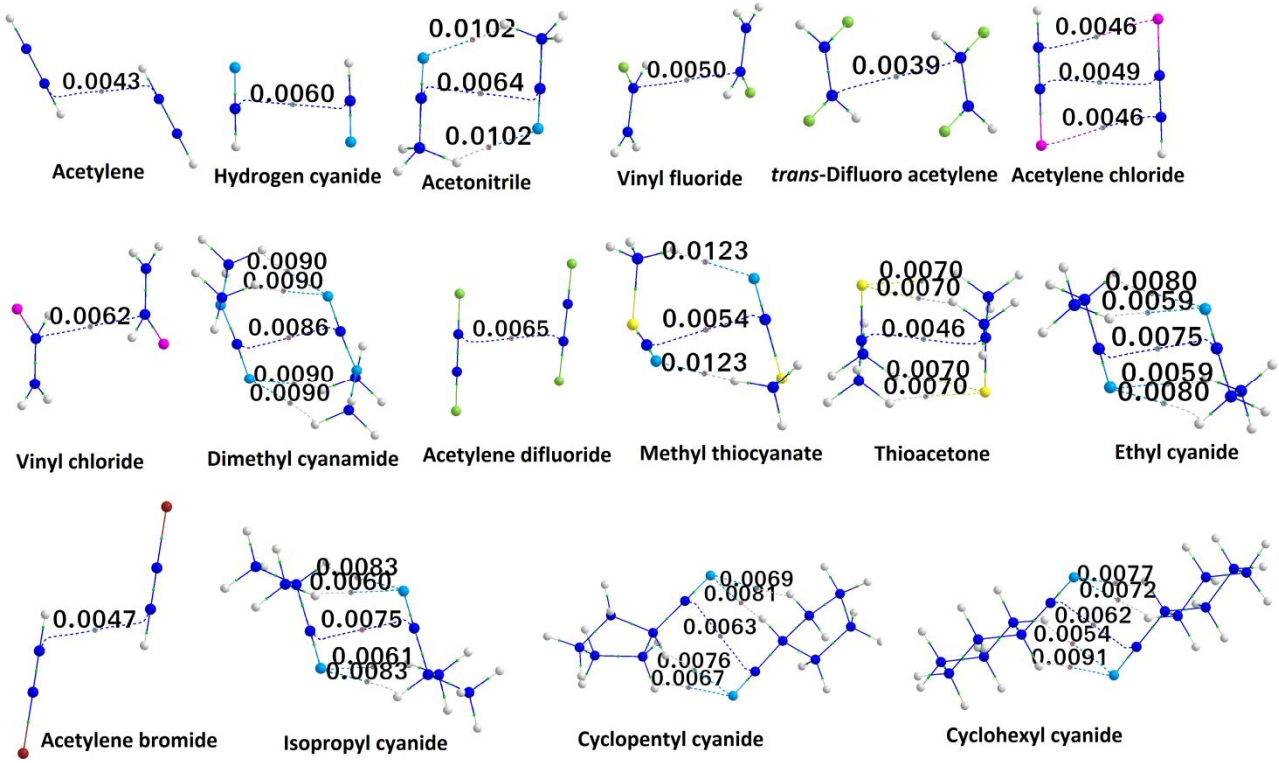


**Figure 2.** AIM plots of the dimers showing Cé C interaction between similar carbon atoms. The ȷ values at the bond critical point are given in au. Color code for atoms: dark blue, carbon; light blue, nitrogen; light green, fluorine; yellow, sulfur; pink, chlorine; brown, bromine; ash, hydrogen

and oxygen atoms of similar chemical environments. Intermolecular chalcogené chalcogen interactions are previously described in literature[13, 34] as leading to the formation of tubular structures[12, 35] and crystals[36].

## Computational Methods

All the molecules are optimized using M06L[37] density functional

theory. The basis set used is 6-311++g(d,p). This model chemistry was previously shown to be suitable in calculating both geometry and interaction energy of non-covalently bound dimers in an extensive benchmark study[38] carried out by us. All the dimers are confirmed to be minima by calculating the frequency. The calculations are done using *Gaussian09*[39] suite of programs. Interaction energy ($E_{int}$) is calculated by subtracting twice the energy of the constituent monomer from the energy of a dimer. The monomers are also optimized at the same level. Counterpoise correction is done using Boys and Bernardi[40] method as implemented in *Gaussian09*. Further validation of the results is done using B3LYP, CAM-B3LYP[41] - the long range corrected version of B3LYP[42] - and B971[43] functionals. To assess the effect of dispersion, B3LYP-D3 method is also employed which uses Grimmeôs dispersion correction along with Becke-Johnson damping function[44]. The basis set used for all these calculations is 6-311++g(d,p). Further, the high accuracy G3MP2[45] method is used to get accurate binding energy values for the dimers.

Atoms-in-molecule (AIM) analysis[46] considers the distribution of electronic charge of atoms in the field of nuclei and its interference with external fields. In this method, critical points in topology of the charge density are related to physical information like bonds. The programs used are AIM2000[47-49] and AIMALL[50]. AIMALL generated molecular graphs are used in the manuscript for illustrating the bonding interactions. MO analysis was done to confirm the bonding interactions corresponding to the intermolecular bond critical points shown by the AIM analysis. Molecular electrostatic potential (MESP), defined by equation (1) can be used as a tool for understanding intermolecular interactions[51-54]. It directly reflects the charge distribution in the system, based upon Coulombôs law[55]. The molecular electrostatic potential at a point **r**, $V(\mathbf{r})$ is given as,

$$V(\mathbf{r}) = \sum_{A}^{N} \frac{Z_A}{|\mathbf{r} - \mathbf{R}_A|} - \int \frac{ƒ(\mathbf{r}')d^3r'}{|\mathbf{r} - \mathbf{r}'|} \qquad (1)$$

where $Z_A$ is the nuclear charge and $R_A$ is the radius of nucleus A and $ƒ(\mathbf{r}')$ is the electron density.

Energy Decomposition Analysis[56-58] (EDA) is done using ADF software[59-61]. In the Morokuma scheme of EDA[62], the interaction energy will be split into Pauli, Electrostatic and orbital contributions. For this, all the dimers were optimized using M06L/tzvp method and single point fragment analysis was done using M06L/tz2p method available in ADF. Some molecules from literature located with the help of Cambridge structural database[63] are shown to have intermolecular Cé C interactions with the help of AIM analysis using AIMALL. Dimers from their crystal structures were chosen and were subjected to single point analysis at M06L/6-311++G(d,p) DFT for the presence of such interactions

Natural bond orbital (NBO) analysis[64] as implemented in *Gaussian09* is used for studying the nature of charge transfer between the two X atoms under study. In this method, the total electronic wavefunction is interpreted in terms of a set of filled Lewis and a set of empty non-Lewis localized orbitals. Using a second order perturbation theory, interaction between these two sets of orbitals resulting in a donation of occupancy from the occupied Lewis to unoccupied non-Lewis set of orbitals is analyzed. This results in the departure from the idealized Lewis structure description. For each pair of donor (*i*) and acceptor (*j*) NBOs, the stabilization energy $E_2$ associated with *i* Ÿ *j* delocalization is calculated as

$$E_2 = \Delta Eij = qi \frac{F(i,j)^2}{\varepsilon j - \varepsilon i} \qquad (2)$$

where qi is the donor orbital occupancy, Ůi, Ůj are diagonal elements (orbital energies) and F(i,j) is the off-diagonal NBO Fock matrix element.

## Results and Discussion

**Intermolecular C…C interaction between carbon atoms in similar chemical environment**

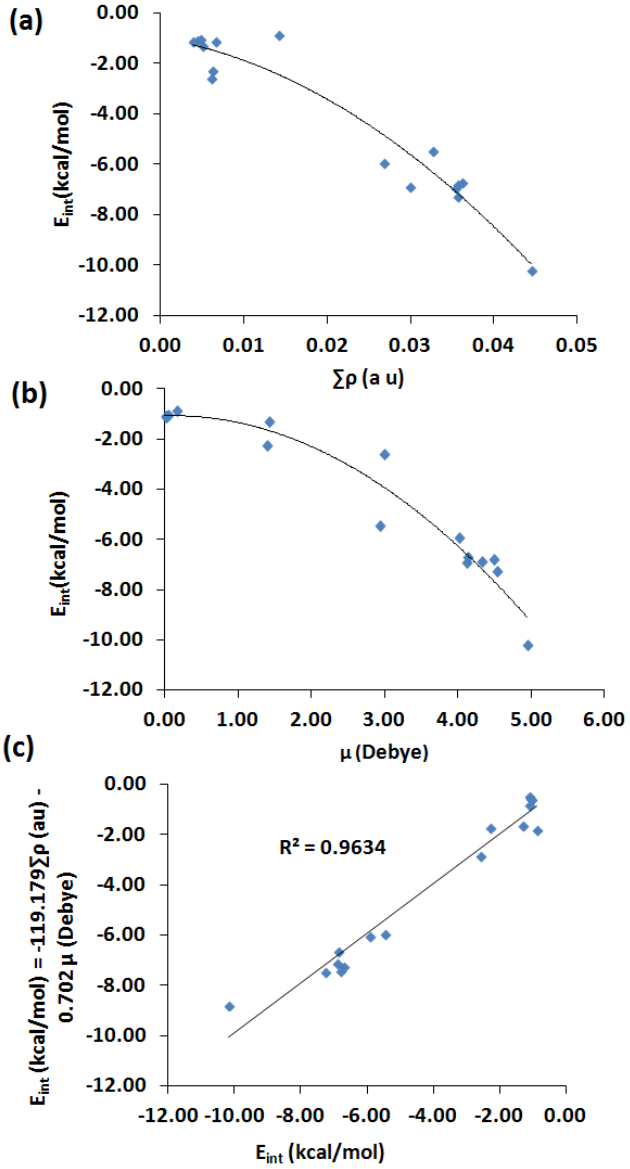


**Figure 3.** Variation of interaction energy ($E_{int}$) with (a) sum of electron density at in intermolecular BCPs (×ƒ), (b) monomer dipole moments (ε) and (c) predicted values of $E_{int}$ using regression equation

The selected systems for this study include triple bonded systems

such as acetonitrile and its derivatives, cycloalkanes with cyanide functional group, dimethyl cyanamide, acetylene and its halogenated derivatives. Double bonded compounds such as ethylene derivatives, methyl thiocyanate and thioacetone are also included in the study. The optimized structures of their dimers are shown in Figure 1. This figure also depicts one intermolecular

**Table 1.** The interaction energies ($E_{int}$), the sum of ρ at inter molecular BCPs (×ρ), and monomer dipole moments (ε) of all the dimers with intermolecular Cé C interaction between similar carbon atoms. The predicted values of $E_{int}$ using regression equation along with contributions from ×ρ and ε terms are also given.

| Dimer | $E_{int}$ (kcal/mol) | ×ρ (a u) | ε (Debye) | Predicted $E_{int}$ (kcal/mol) | Contribution from ×ρ (kcal/mol) | Contribution from ε (kcal/mol) |
|---|---|---|---|---|---|---|
| acetylene | -1.07 | 0.0043 | 0.00 | -0.51 | -0.51 | 0.00 |
| hydrogen cyanide | -2.59 | 0.0060 | 2.98 | -2.81 | -0.72 | -2.09 |
| acetonitrile | -5.93 | 0.0268 | 4.01 | -6.01 | -3.19 | -2.81 |
| ethyl cyanide | -6.91 | 0.0353 | 4.11 | -7.09 | -4.21 | -2.88 |
| isopropyl cyanide | -6.70 | 0.0361 | 4.13 | -7.20 | -4.31 | -2.90 |
| cyclopentyl cyanide | -6.79 | 0.0356 | 4.48 | -7.38 | -4.24 | -3.14 |
| cyclohexyl cyanide | -7.27 | 0.0356 | 4.52 | -7.41 | -4.24 | -3.17 |
| dimethyl cyanamide | -10.19 | 0.0445 | 4.94 | -8.77 | -5.30 | -3.47 |
| vinyl flouride | -1.29 | 0.0050 | 1.42 | -1.59 | -0.60 | -0.99 |
| vinyl chloride | -2.27 | 0.0062 | 1.39 | -1.71 | -0.74 | -0.97 |
| *trans*- difluoro ethylene | -1.09 | 0.0039 | 0.01 | -0.47 | -0.46 | -0.01 |
| actylene chloride | -0.87 | 0.0141 | 0.16 | -1.79 | -1.68 | -0.11 |
| acetylene bromide_2 | -1.03 | 0.0047 | 0.03 | -0.59 | -0.56 | -0.02 |
| acetylene difluoride | -1.12 | 0.0065 | 0.00 | -0.77 | -0.77 | 0.00 |
| methyl thiocyanate | -6.88 | 0.0299 | 4.32 | -6.59 | -3.56 | -3.03 |
| thioacetone | -5.45 | 0.0326 | 2.92 | -5.94 | -3.89 | -2.05 |

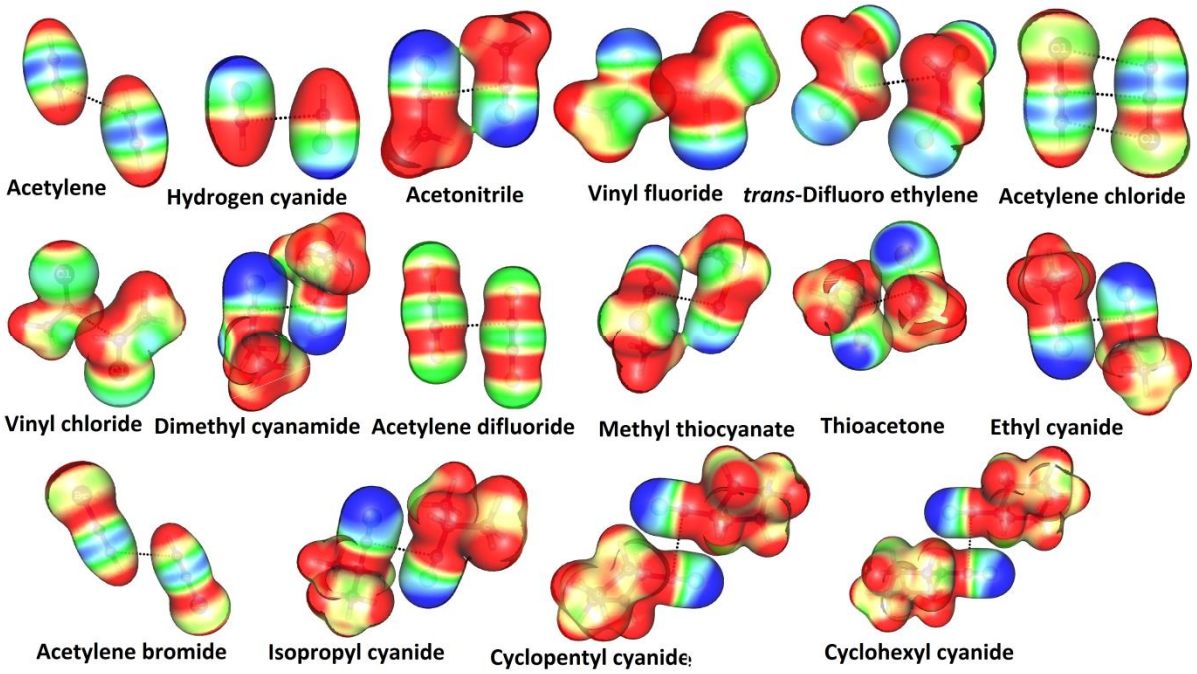


**Figure 4.** MESP plotted on isodensity surface of 0.01 au of dimers showing Cé C interaction between similar carbon atoms. Range: from -0.03 (blue) to 0.05 (red).

Cite this: DOI: 10.1039/c0xx00000x

www.rsc.org/xxxxxx

ARTICLE TYPE

**Table 2.** Percentage orbital and electrostatic contributions towards the total interaction energy of the dimers with intermolecular Cé C interactions.

| Dimer | % Electrostatic Interaction | % Orbital Interaction |
|---|---|---|
| Acetylene | 92.74 | 7.26 |
| Hydrogen cyanide | 95.86 | 4.14 |
| Acetonitrile | 85.13 | 14.87 |
| Ethyl cyanide | 82.13 | 17.87 |
| Isopropyl cyanide | 80.83 | 19.17 |
| Cyclopentyl cyanide | 80.94 | 19.06 |
| Cyclohexyl cyanide | 76.96 | 23.04 |
| Dimethyl cyanamide | 78.11 | 21.89 |
| Vinyl fluoride | 67.81 | 32.19 |
| Vinyl chloride | 75.25 | 24.75 |
| *trans*-difluoro ethylene | 65.79 | 34.21 |
| Acetylene chloride | 33.33 | 66.67 |
| Acetylene bromide | 72.31 | 27.69 |
| Acetylene difluoride | 83.33 | 16.67 |
| Methyl thiocyanate | 78.44 | 21.56 |
| Thioacetone | 60.37 | 39.63 |

Cé C interaction distance for every dimer. Later it will be revealed that this Cé C interaction is brought out in terms of identifying a bonding molecular orbital (MO) as well as by locating a bond critical point in the AIM analysis. Dimers of hydrogen cyanide, acetylene derivatives except acetylene chloride and ethylene derivatives show only Cé C interactions between their monomers. Acetylene chloride dimer shows carbon-halogen interactions along with Cé C interaction. Cyanides, cyanamides, thiocyanate and thioacetone show hydrogen bonding interactions apart from Cé C interactions.

Herein we focus mainly on the Cé C interactions. The carbon atoms participating in this interaction are from similar chemical environment and their Cé C distances are in the range 3.10 ï 3.62 Å. This range of distance does not indicate a significant bonding interaction between them. However, the bonding MO analysis and the AIM electron density analysis suggest a new view point. This Cé C interaction is not a donor ï acceptor type interaction (the ódicarbon bondô described by Varadwaj *et al*[28]) because the interacting carbons atoms are from similar chemical environment and hence neither of them can be described as donor or acceptor. All the dimers showing this type of Cé C interactions possess double or triple bonds either in the functional group or in the main chain. We could not locate any saturated compounds such as alcohols, amines, alkyl halides and thiols showing similar Cé C interaction.

The bonding MO (supporting information) of every dimer complexes clearly show interaction between the p orbitals of the carbon atoms in the similar chemical environment. In cases such as hydrogen cyanide, dimethyl cyanamide and acetylene difluoride, the orbital overlap is stronger compared to others. The AIM plots given in Figure 2 show a bond critical point for every Cé C interaction depicted in Figure 1. The electron density at intermolecular BCPs is often used as a measure of the strength of intermolecular interactions[33, 65-68]. The ɟ values (0.0039 to 0.0086 au) given in Figure 2 for the Cé C interactions are well within the typical values observed for weak non-covalent interactions such as weak hydrogen bonds[67, 69] and ócarbon bondsô[19]. Among all the cases, *trans*ï difluoro ethylene (ɟ = 0.0039 au) has the weakest and dimethyl cyanamide (ɟ = 0.0086 au) has the strongest Cé C interactions. The values of $E_{int}$, sum of ɟ at intermolecular BCPs (×ɟ), and monomer dipole moments (µ)of all the dimers are given in Table 1.

The ×ɟ is generally used to assess the total strength of the non-covalent interaction in intermolecular complexes[33, 70-71]. The interaction energy ($E_{int}$) shows an increasing trend with increase in the ×ɟ values (Figure 3. (a)). Recently, Mohan and Suresh[54] showed that a correlation between ɟ and interaction energy is applicable only for homogenous groups of complexes. The $E_{int}$ is also found to increases with increase in the dipole moment ε of the molecule (Figure 3. (b)). Since both ×ɟ and ε show dependency to $E_{int}$ values, a double linear regression approach using the two quantities is tried to obtain a relationship to predict $E_{int}$ values. The regression equation is given in eq. (2). The statistical parameters such as multiple R and $R^2$ are 0.9937 and 0.9875 respectively. The P values for ×ɟ and ε are 7.9781 ‰$10^{-5}$ and 0.0013 respectively, suggesting that eq.(2) is trustworthy. The predicted and actual values deviate only slightly (Ò 0.92 kcal/mol) except for dimethyl cyanamide where the deviation is 1.4 kcal/mol (Figure 3(c)).

$$E_{int}\ (\text{kcal/mol}) = -119.179 \times ɟ\ (\text{au}) - 0.702\ ε\ (\text{Debye}) \qquad (3)$$

Eq. (2) allows us to separate $E_{int}$ into contributions from ×ɟ and ε which are also depicted in Table 1. In the cases of hydrogen cyanide, vinyl fluoride and vinyl chloride dimers, where a Cé C interaction is the only intermolecular interaction between the monomers, 57 - 75% of the $E_{int}$ is contributed from the dipole moment term. For cyanides, dimethyl cyanamide, methyl cyanate, and thioacetone, where hydrogen bonding interactions also contribute towards $E_{int}$, the contribution from the dipole moment term is 35 ï 47%. For compounds with very low or even zero dipole moment, the contribution from the dipole moment term is very low (0 ï 6%).

The plot of molecular electrostatic potential (MESP) of the dimers are given in Figure 4. Based on the MESP features of the dimers, a partitioning of their monomers into electron deficient (red) and electron rich (blue) regions can be easily recognized and this immediately suggests that electron rich region of one of the monomers is close to electron deficient region of the other resulting in an antiparallel arrangement. This can be clearly

Cite this: DOI: 10.1039/c0xx00000x

www.rsc.org/xxxxxx

ARTICLE TYPE

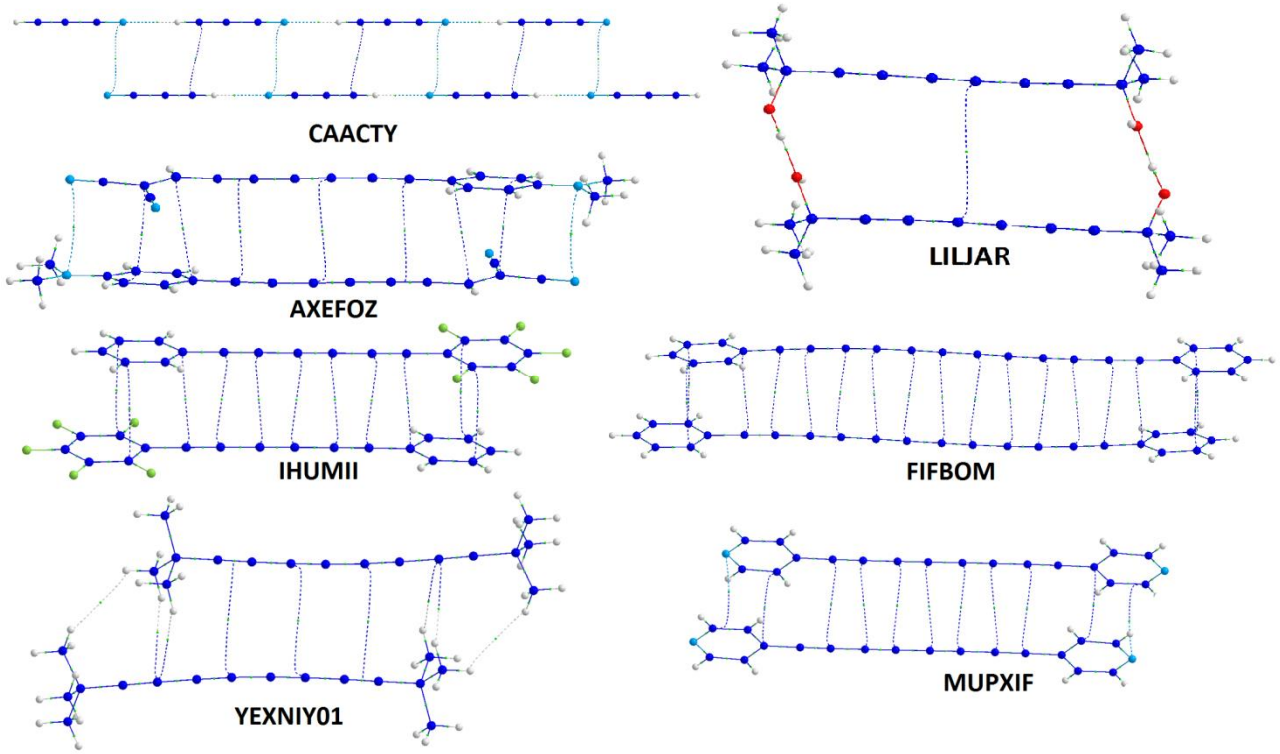


**Figure 5.** AIM plot of dimers obtained from crystal structures reported in the literature. The CSD ID is used for labeling. Color code for atoms: dark blue, carbon; light blue, nitrogen; red, oxygen; light green, fluorine; ash, hydrogen.

illustrated in all the cases, most visibly, in cases of cyanides and cyanamide. It is also clear that though the C atoms involved in the Cé C interactions are from similar chemical environment, they are the sites of transition of electrostatic potential from negative (electron rich) to positive (electron deficient) values. In fact, MESP plots indicate that nearly one half of such a carbon is electron rich and the other half is electron deficient. The approach of the electron rich region of such a carbon in one monomer to the electron deficient region of another carbon in the second monomer results in Cé C bonding between carbon atoms in similar chemical environment. In acetylene and its derivatives, though the dipole moment is zero or nearly zero for the monomer state, local variations in MESP in the dimer is significant due to polarization effects which cause Cé C interactions.

Energy decomposition analysis (EDA) shows that the interaction energies of these dimers, are mainly electrostatic in nature (Table 2). Electrostatic contribution towards $E_{int}$ is the highest (95.86%) in the case of hydrogen cyanide dimer, where a Cé C interaction is the only intermolecular interaction and has a high monomer dipole moment. Though μ value is zero, higher electrostatic contribution towards $E_{int}$ in acetylene (92.74%) and difluoro acetylene (83.33%) show that electrostatic effects due to local polarization leads to these interactions. The Coulombic interactions encompass polarization (and accordingly include dispersion) as a consequence of Hellmann-Feynman theorem[72].

For the dimers such as acetonitrile and its derivatives, dimethyl cyanamide and thioacetone, where hydrogen bonds also contribute towards $E_{int}$, 60 - 85% of it is from electrostatic contribution

**Evidence for C…C interaction between carbon atoms in similar chemical environments from crystal structures**

We have located a few molecules with intermolecular Cé C interaction between carbon atoms in similar chemical environment in the literature with the help of Cambridge structural database (CSD). The AIM plots labelled with their CSD ID given in Figure 5 show all the intermolecular interactions. CAACTY,[73] is the crystal structure of acetylene cyanide. It shows intermolecular Cé C interactions between chemically identical carbon atoms. Polyynes with different end groups are located to have intermolecular Cé C interactions in their crystal structures. The intermolecular Cé C interaction in LILJAR[74] and the central Cé C interactions in the case of AXEFOZ[75], FIFBOM[76], IHUMII[77], MUPXIF,[78] and YEXNIY01[79] are also between carbon atoms from identical environments. In the remaining Cé C interactions, though the carbon atoms involved are not of the same types, many of them can be considered as of similar types. Apart from Cé C

interactions and hydrogen bonds, the acetylene cyanide crystal (CAACTY) also shows BCPs corresponding to Né N interaction

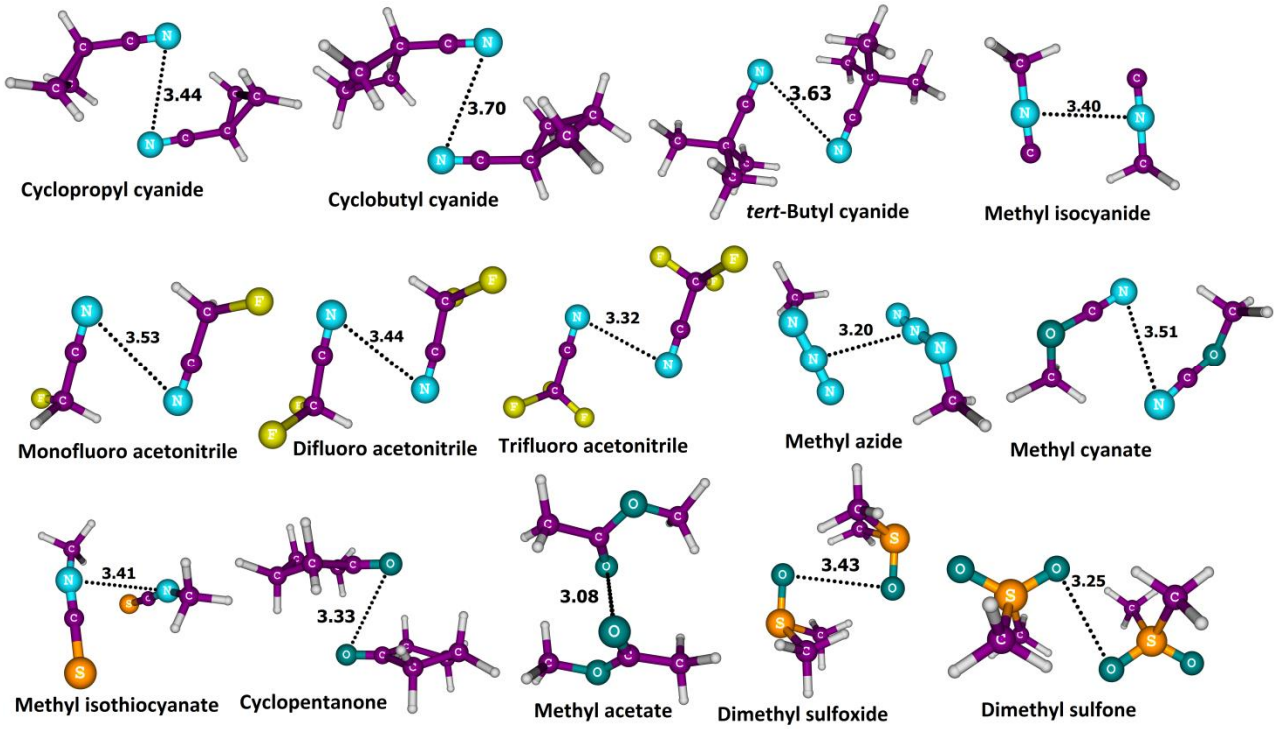


**Figure 6.** Dimers showing Né N and Oé O interaction between similar atoms. Distances are in Å

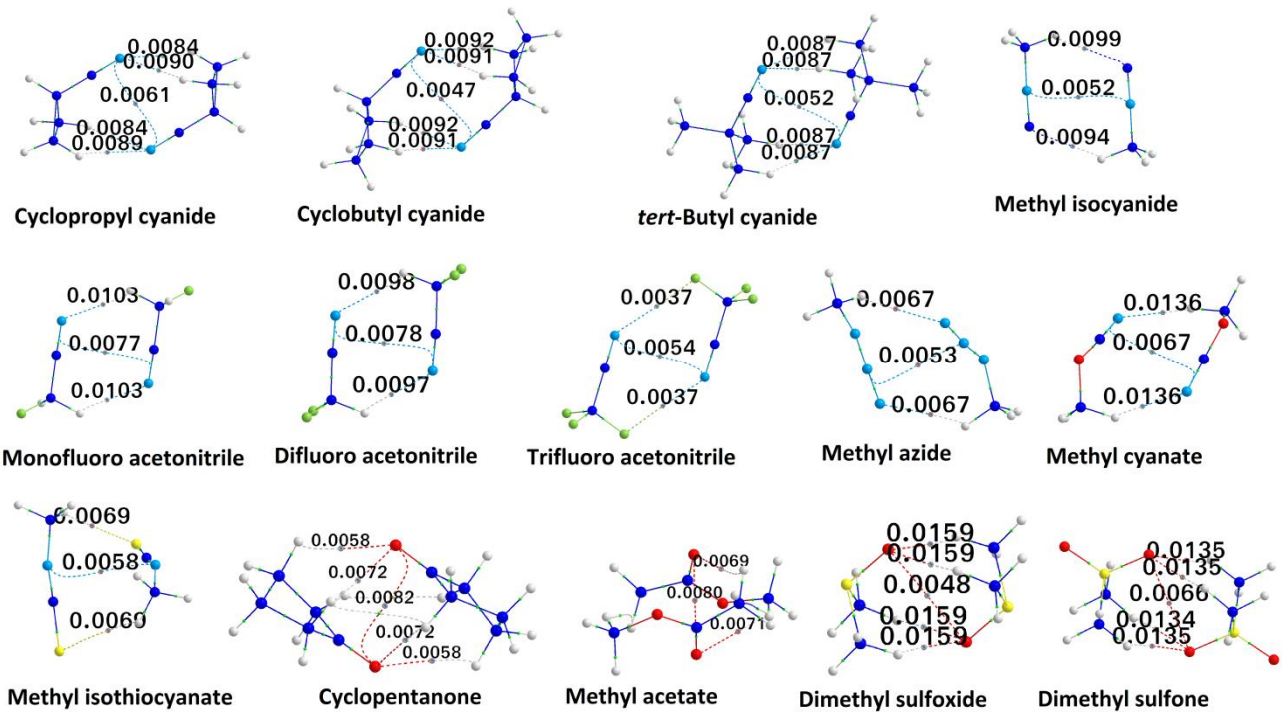


**Figure 7.** AIM plots of the dimers showing Né N and Oé O interaction between similar atoms. The intermolecular BCPs are given in au. Color code for atoms: dark blue, carbon; light blue, nitrogen; red, oxygen; light green, fluorine; yellow, sulfur; ash color, hydrogen

Cite this: DOI: 10.1039/c0xx00000x

www.rsc.org/xxxxxx

ARTICLE TYPE

**Table 3.** The interaction energy ($E_{int}$), sum of ɟ at inter molecular BCPs (×ɟ), and monomer dipole moment (ε) of dimers with Né N and Oé O interactions

| Dimer | $E_{int}$ (kcal/mol) | ×ɟ (a u) | ε (Debye) | Predicted $E_{int}$ (kcal/mol)(from eq. (2) |
|---|---|---|---|---|
| cyclopropyl cyanide | -7.6 | 0.0407 | 4.39 | -7.93 |
| cyclobutyl cyanide | -7.74 | 0.0413 | 4.35 | -7.97 |
| tert - Butyl cyanide | -6.73 | 0.0399 | 4.11 | -7.64 |
| Monofluoro acetonitrile | -6.06 | 0.0284 | 3.21 | -5.64 |
| Difluoro acetonitrile | -5.48 | 0.0273 | 2.38 | -4.92 |
| Trifluoro acetonitrile | -1.53 | 0.0128 | 1.24 | -2.40 |
| methyl isocyanide | -4.84 | 0.0246 | 3.88 | -5.65 |
| methyl azide | -3.41 | 0.0188 | 2.47 | -3.97 |
| methyl cyanate | -8.69 | 0.0339 | 4.66 | -7.31 |
| Methyl isothiocyanate | -4.45 | 0.0196 | 3.12 | -4.52 |
| Cyclopentanone | -7.68 | 0.0408 | 3.14 | -7.07 |
| Methyl acetate | -5.14 | 0.0292 | 1.83 | -4.76 |
| Dimethyl sulfoxide | -12.03 | 0.0682 | 4.12 | -11.02 |
| Dimethylsulfone | -11.26 | 0.0605 | 4.57 | -10.42 |

between nitrogen atoms of similar chemical environment. This fact points to the possibility of extending the concept of interaction between atoms in similar chemical environments to atoms other than carbon.

**Intermolecular N…N and O…O interactions**

The studied dimer systems for the analysis of Né N and Oé O interaction in similar chemical environment are given in Figure 6 along with their Né N and Oé O bonds marked in dotted lines. These include dimers of compounds with functional groups such as cyanides, (acetonitrile derivatives and cycloalkanes with cyanide functional group), isocyanide, azide, cyanate and isothiocyante. The oxygen containing compounds studied include a cyclic ketone, an ester, a sulfoxide and a sulfone dimer. The bond lengths vary from 3.20 to 3.70 Å for Né N interactions and 3.08 to 3.48 Å for Oé O interactions. The AIM plots of these dimers give BCPs corresponding to Né N and Oé O interaction (Figure 7). The values of $E_{int}$, ×ɟ and ε of all the complexes are given in Table 3. The range of ɟ values at Né N BCPs is from 0.0047 to 0.0078 au and at Oé O BCPs is from 0.0043 to 0.0082 au. $E_{int}$ values of dimers with Né N as well as Oé O interactions increase with increase in the values of ×ɟ and ε (supporting information). In order to check the validity of the assumption that the concept of intermolecular interaction between atoms in similar chemical environments is atom independent, eq (2)

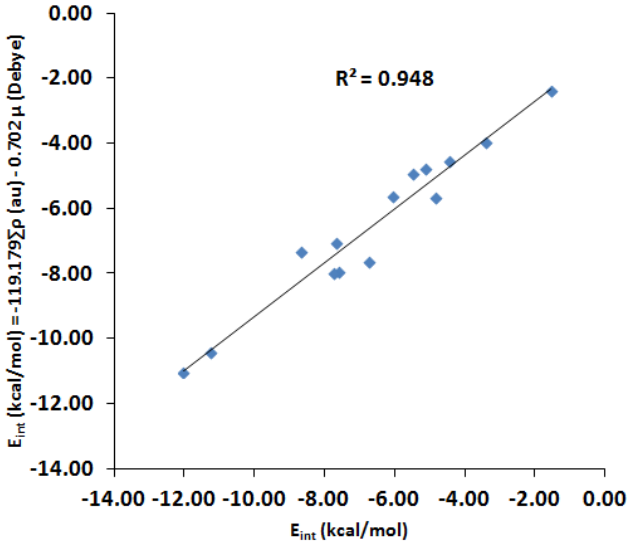


**Figure 8.** Correlation of $E_{int}$ with $E_{int}$ values predicted using eq. (2) for complexes showing Né N and Oé O interactions

(obtained strictly for dimers with Cé C interactions) is used for predicting the values of $E_{int}$ of the complexes with Né N and Oé O interactions. The predicted values of $E_{int}$ are given in Table 3 which show good agreement with the actual $E_{int}$ values (Figure 8) (the deviation is < 1 kcal/mol for all except methyl cyanate and

Cite this: DOI: 10.1039/c0xx00000x

www.rsc.org/xxxxxx

ARTICLE TYPE

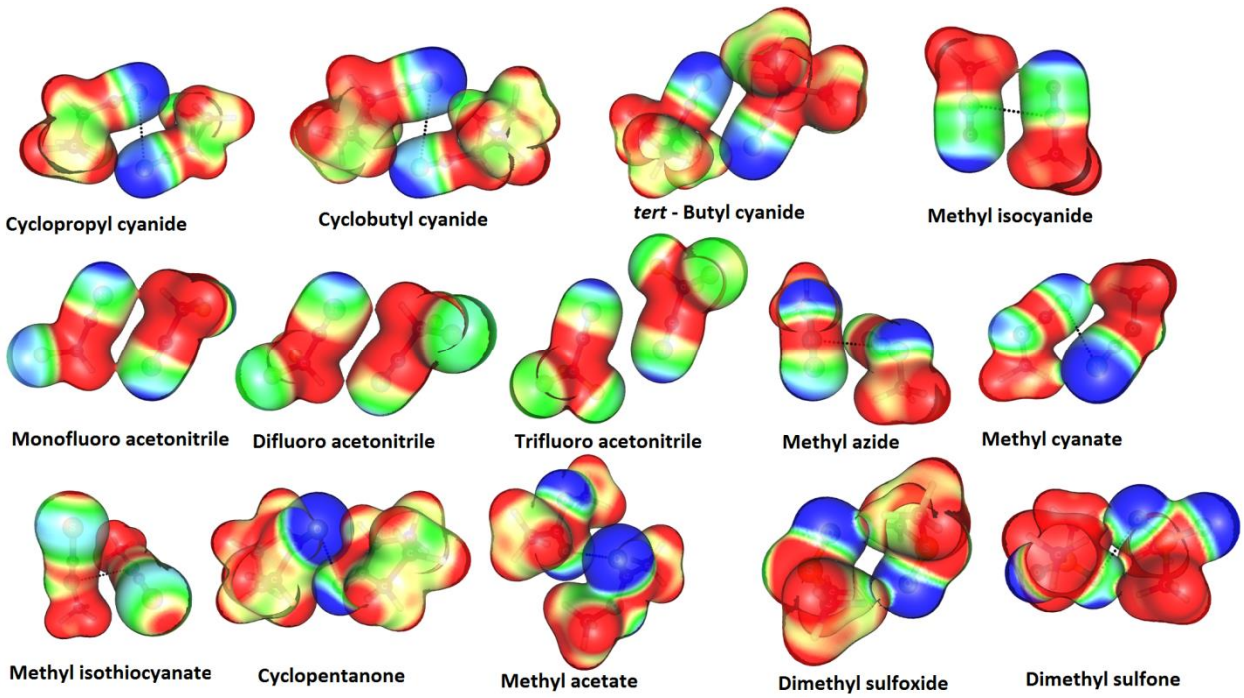


**Figure 9.** MESP plotted on isodensity surface of 0.01 au of dimers showing Né N and Oé O interaction between similar atoms. Range: from -0.03 to 0.05 from blue to red

dimethyl sulfoxide, where the deviation is 1.38 and 1.01 kcal/mol respectively). As in the case of complexes with Cé C interaction between similar atoms, the geometry of the complexes with Né N and Oé O interactions are also driven by the dipole moments of their constituent monomers which can be figured out from their MESP plots (Figure 9). Local variations in charge density due to polarization effects cause similar atoms with antiparallel orientation to participate in bonding interaction. In Figure S10 of the supporting information, MESP map plotted on 0.001 au electron density surface (MESP range -0.03 to 0.03 au) of dimers of some of the typical cases of Cé C, Né N and Oé O interactions are shown along with those of the corresponding monomers. This figure shows that significant charge redistribution occurs on monomer units upon dimer formation. Occupied MOs corresponding to Cé C, Né N and Oé O noncovalent bonds are also located for all the dimer systems (supporting information).

The EDA data for complexes with Né N and Oé O interaction between similar atoms is given in Table 4. Here, similar to the case of complexes with Cé C interactions, the electrostatic contribution to the values of $E_{int}$ is found to be very high (62.52 ï 88.73%)

**NBO analysis**

In relation with each X1é X2 interaction, NBO analysis shows charge transfer from orbitals on X1 atom to those on X2 atom and similar charge transfer from orbitals on X2 to orbitals on X1, with the $E_2$ values for both the charge transfers being similar. This observation supports the assumption that X atoms involved in an Xé X interaction serve both as donor and as acceptor. For instance, in acetylene dimer, the interaction between C2 atom on molecule 1 with C6 atom on molecule 2 corresponds to a charge transfer from the bonding orbitals on C2 to antibonding and RY* orbitals on C6 with $E_2$ values indicating a stabilizing interaction (sum of $E_2$ values = 0.84 kcal/mol). Similar charge transfer interactions from the bonding orbitals on C6 to antibonding and RY* orbitals on C2 with same values of $E_2$ are also observed. $E_2$ values of charge transfers corresponding to each intermolecular interaction in acetylene and acetonitrile dimers are given in the supporting information as typical examples. A charge transfer from lone pairs or bonding orbitals to antibonding (BD*) orbital occurs in Xé X interactions in almost all case except in trifluoroacetonitrile, methyl azide and dimethyl sulfoxide, where the acceptor orbitals are mainly RY* orbitals. Charge transfer corresponding to Xé X interactions shown by AIM analysis are located in almost all the cases. The orbitals involved in these charge transfer interactions are shared by the X atoms in all cases except in trifluoroacetonitrile (Né N) and dimethylsulfone (Oé O). In trifluoroacetonitrile, where AIM analysis indicates Né N interaction, the charge transfer occurs from bonding orbitals on one N atom to the RY* orbital on C near to the N atom. Similarly, in dimethyl sulfone, the O2é O12 interaction shown in AIM analysis involves a charge transfer from the lone pair on O2 to antibonding orbital on the S atom next to O12. A

similar charge transfer occurs from the lone pair on O12 to the antibonding orbital on the S atom next to O2 with an equal value of $E_2$.

The summed up values of $E_2$ corresponding to all the interactions in the dimers is listed in Table 5. In many cases such as ethyl cyanide, isopropyl cyanide and dimethyl cyanamide, the total value of $E_2$ corresponding to Cé C interaction is larger than that corresponding to the individual hydrogen bonds (HB). But in cases such as dimethyl sulfoxide and dimethyl sulfone, the $E_2$ value corresponding to Oé O interaction is very less compared to that of the individual hydrogen bonds. However, in all the cases, the total stabilization obtained via hydrogen bonds is much higher compared to that by Xé X interactions. Thus, the geometry of the dimers must be driven by stronger interactions such as hydrogen bonds with Xé X interactions being a further stabilizing effect for such geometry. This can be shown in our study of growth patterns in acetonitrile clusters[33] where, the stacked clusters, with the highest possible number of C-Hé N interactions, is further stabilized by Cé C interactions between antiparallelly arranged monomers. In cases such as trifluoroacetonitrile and dimethylsulfone, where AIM analysis indicates Né N and Oé O interactions respectively, the NBO analysis shows charge transfer from the orbitals shared by one N/O atom to the orbitals on the atoms next to second N/O atom instead of the second N/O atom. This indicates that the bond paths and BCPs in the AIM analyis should not be taken too literally[80-81] and that the entire regions in the two molecules may be interacting.

**Validation of the results using statistical methods**

It is remarkable that the equation designed for dimers with Cé C interactions (eq. 2) is useful to predict the $E_{int}$ values of those with Né N and Oé O interactions with a good degree of accuracy. This suggests that the dipole enforced interaction could be a general phenomenon. Considering the data on Cé C, Né N and Oé O interactions, a more general equation to predict $E_{int}$ can be obtained using linear regression on ×Ɉ and ε (eq 3).

$E_{int}$ (kcal/mol) = -138.395×Ɉ (au) ï 0.551ε (Debye) (3)

There is a good correlation between $E_{int}$ values obtained using eq. 3 and the actual $E_{int}$ of all the complexes as given in Figure 10. The values of statistical parameters *viz.* multiple R and $R^2$ are 0.9950 and 0.9900 respectively. The P values for ×Ɉ and ε are 1.8 ঌ$10^{-12}$ and 3.03 ঌ$10^{-5}$ respectively, indicating that eq. (3) is reliable.

**Table 4.** Percentage orbital and electrostatic contributions towards the total interaction energy of the dimers with Né N and Oé O interactions between similar atoms

| Dimer | % Electrostatic Interaction | % Orbital Interaction |
|---|---|---|
| cyclopropyl cyanide | 79.64 | 20.36 |
| cyclobutyl cyanide | 73.95 | 26.05 |
| *tert* - Butyl cyanide | 75.77 | 24.23 |
| Monofluoro acetonitrile | 82.17 | 17.83 |
| Difluoro acetonitrile | 84.22 | 15.78 |
| Trifluoro acetonitrile | 88.73 | 11.27 |
| methyl isocyanide | 83.90 | 16.10 |
| methyl azide | 87.90 | 12.10 |
| methyl cyanate | 80.03 | 19.97 |
| Methyl isothiocyanate | 69.05 | 30.95 |
| cyclopentanone | 69.00 | 31.00 |
| methyl acetate | 70.79 | 29.21 |
| Dimethyl sulfoxide | 70.14 | 29.86 |
| Dimethylsulfone | 74.05 | 25.95 |

**Table 5.** Total $E_2$ values in kcal/mol corresponding to each interactions in the dimers

| Dimer | Xé X | HB1[#] | HB2 | HB3 | HB4 |
|---|---|---|---|---|---|
| Acetylene | 0.84 | - | - | - | - |
| HCN | 1.39 | - | - | - | - |
| Acetonitrile | 1.04 | 1.76 | 1.76 | | |
| Ethyl cyanide | 1.25 | 0.28 | 0.12 | 0.28 | 0.12 |
| Isopropyl cyanide | 1.12 | 0.33 | 0.13 | 0.38 | 0.08 |
| Cyclopentyl cyanide | 0.69 | 0.29 | 0.41 | 0.15 | 0.21 |
| Cyclohexyl cyanide | 0.61 | 0.08 | 0.70 | 0.37 | 0.27 |
| Dimethyl cyanamide | 1.88 | 0.76 | 0.76 | 0.76 | 0.76 |
| Vinyl fluoride | 0.52 | - | - | - | - |
| Vinyl Chloride | 1.00 | - | - | - | - |
| *trans* - Difluoro ethylene | 0.14 | - | - | - | - |
| Acetylene chloride | 0.58 | 0.41 | 0.41 | - | - |
| Acetylene bromide | 0.88 | - | - | - | - |
| Acetylene difluoride | 0.75 | - | - | - | - |
| Methyl thiocyanate | 0.32 | 3.04 | 3.04 | - | - |
| Thioacetone | 0.74 | 0.90 | 0.90 | 0.90 | 0.90 |
| Cyclopropyl cyanide | 0.15 | 0.57 | 0.71 | 0.74 | 0.58 |
| Cyclobutyl cyanide | 0.18 | 0.99 | 1.02 | 0.99 | 1.02 |
| *tert* - Butyl cyanide | 0.22 | 1.2 | 1.2 | 1.21 | 1.2 |
| Monofluoroacetonitrile | 0.5 | 1.42 | 1.43 | - | - |
| Difluoroacetonitrile | 0.56 | 1.38 | 1.4 | - | - |
| Trifluoroacetonitrile | 0.24 | 0.13 | 0.13 | - | - |
| Methyl isocyanide | 0.16 | 1.8 | 1.99 | - | - |
| Methyl azide | 0.61 | 0.54 | 0.62 | - | - |
| Methyl cyanate | 0.22 | 3.6 | 3.56 | - | - |
| Methyl isothiocyanate | 0.14 | 1.91 | 1.92 | - | - |
| Cyclopentanone | 1.47 | 0.19 | 0.18 | 0.2 | 0.18 |
| Methyl acetate | 0.64 | 0.23 | 0.25 | 0.07 | - |
| Dimethyl sulfoxide | 0.14 | 3.67 | 3.67 | 3.67 | 3.67 |
| Dimethyl sufone | 0.2 | 3.07 | 3.02 | 3.01 | 3.04 |

[#]HB indicates Cé Cl interaction in acetylene chloride Né F interaction in trifluoroacetonitrile and hydrogen bonds in all other cases.

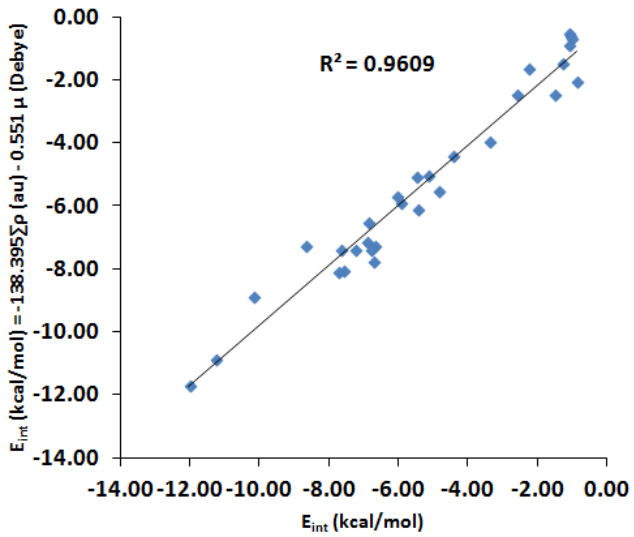


**Figure 10.** Correlation of $E_{int}$ with predicted values of $E_{int}$ using eq. (3) for all the complexes with Cé C, Né N and Oé O interaction between atoms in similar chemical environments

Further validation of the results is done using ódeave one outô method of statistical analysis. This is done by predicting the $E_{int}$ values of all except one dimer from the entire set of dimers from their ×Ɉ and ε values using double linear regression analysis. From the equation thus obtained, the $E_{int}$ value of the exempted dimer is calculated. The process is repeated and $E_{int}$ value of each dimer is predicted from the equation obtained for the remaining ones. The values thus predicted show very good agreement with the actual $E_{int}$ values ($R^2$ = 0.9554, supporting information). The method also provides a set of regression equations. It is observed that the coefficients of ×Ɉ (range between -133.170 and -143.577) and ε (range between -0.490 and -0.592) do not show much variation. The values of coefficients of ×Ɉ lie in between -137 and 139 in most of the cases. Only five out of thirty values are out of this range. Consequently, the $E_{int}$ values predicted by these equations do not show much variation. Thus, the $E_{int}$ values obtained from these equations agree well with each other and with the actual values of $E_{int}$ of the complexes. The thirty equations for predicting $E_{int}$ from ódeave one outô method are given in the supporting information.

**Validation of the results using more density functionals and G3MP2 method**

The $E_{int}$ values obtained at M06L, CAM-B3LYP, B971, B3LYP, B3LYPD3 and G3MP2 Levels of theory are listed in Table 6. Arguably G3MP2 gives the most accurate result on $E_{int}$. However, the geometry obtained from G3MP2 is not reliable because it uses Hartree-Fock level optimized geometry for a subsequent MP2 level optimization. With all the methods, the geometries of some of the dimers deviate from the M06L geometry, which is also indicated in the table with a # mark. However, from our benchmark study where the geometry and $E_{int}$ of small non covalent dimers provided by 382 DFT methods are compared with CCSD values[38], M06L geometries are found to be the most reliable.

The mean absolute deviation (MAD) of the deviation of $E_{int}$ values from G3MP2 values for M06L, B3LYPD3, B3LYP, B971 and CAM-B3LYP are 0.52, 0.57, 0.86, 1.21 and 1.44 respectively, indicating the highest reliability of M06L energies again supporting our benchmark study. M06L and B3LYP-D3 results show close agreement to overall trend and magnitude of the G3MP2 results which is also clear from Table 6. B3LYPD3 shows higher magnitudes of $E_{int}$ compared to B3LYP in all the cases indicating that dispersion effects play an important role in the stability of the dimers. The difference between the two (which range between -0.73 kcal/mol in the case of hydrogen cyanide and -5.53 kcal/mol in the case of dimethyl sulfone) can give an estimate of the effect of dispersion in each dimer. However, a comparison between G3MP2 and B3LYPD3 values indicate that the latter theory slightly overestimate the binding energy.

In order to confirm the reliability of the correlation shown in Figure 10, the $E_{int}$ values of G3MP2 geometries is predicted from ×Ɉ and ε values calculated using CAM-B3LYP, B971 and M06L functionals by double linear regression analysis. The predicted values give a good agreement with the actual $E_{int}$ values (supporting information). $E_{int}$ of the dimers showing considerable deviation from M06L geometry are not included in the regression analysis. CAM-B3LYP and B971 are selected since these methods give the lowest number of geometries deviated from M06L geometry.

Cite this: DOI: 10.1039/c0xx00000x

www.rsc.org/xxxxxx

ARTICLE TYPE

**Table 6.** Values of Eint obtained at different levels of DFT and with G3MP2 method of all the dimers with Xé X interactions.

| Dimer | M06L | CAM-B3LYP | B971 | B3LYP | B3LYPD3 | G3MP2 |
|---|---|---|---|---|---|---|
| Acetylene | -1.07 | -0.37 | -0.89 | -0.73[#] | -1.62[#] | -0.89[#] |
| HCN | -2.59 | -1.39 | -2.29 | -4.22[#] | -4.95[#] | -4.15[#] |
| Acetonitrile | -5.93 | -5.01 | -5.20 | -4.02 | -6.46 | -4.38 |
| Ethyl cyanide | -6.91 | -4.80 | -5.10 | -3.80 | -7.06 | -5.34 |
| Isopropyl cyanide | -6.7 | -4.55 | -4.85 | -3.61 | -6.95 | -5.38 |
| Cyclopentyl cyanide | -6.79 | -4.64 | -5.03 | -3.60 | -7.42 | -5.93 |
| Cyclohexyl cyanide | -7.27 | -4.56 | -4.97 | -3.40 | -7.54 | -6.19 |
| Dimethyl cyanamide | -10.19 | -6.97 | -6.94 | -5.40 | -9.98 | -8.17 |
| Vinyl fluoride | -1.29 | -1.15[#] | -0.73 | -0.31 | -1.96[#] | -0.46[#] |
| Vinyl Chloride | -2.27 | -0.36 | -0.93 | -0.29 | -2.57[#] | -0.83[#] |
| *trans* - Difluoro ethylene | -1.09 | -0.67[#] | -1.65[#] | -1.40[#] | -2.65[#] | -0.63[#] |
| Acetylene chloride | -0.87 | 0.11 | -0.35 | -0.54[#] | -1.53[#] | -0.52 |
| Acetylene bromide | -1.03 | -0.73 | -1.04 | -0.58[#] | -1.94[#] | -0.34 |
| Acetylene difluoride | -1.12 | -0.24 | -0.38 | 0.13 | -1.28 | -0.22 |
| Methyl thiocyanate | -6.88 | -5.50 | -5.13 | -4.63 | -7.74 | -5.63 |
| Thioacetone | -5.45 | -2.06 | -2.98 | -1.22 | -5.83 | -4.24 |
| Cyclopropyl cyanide | -7.6 | -5.17 | -5.57 | -3.94 | -7.46 | -5.55 |
| Cyclobutyl cyanide | -7.74 | -4.85 | -5.32 | -3.57 | -7.77 | -5.86 |
| *tert* - Butyl cyanide | -6.73 | -4.30 | -4.80 | -3.14 | -6.85 | -5.14 |
| Monofluoroacetonitrile | -6.06 | -5.19 | -5.30 | -4.12 | -6.67 | -5.06 |
| Difluoroacetonitrile | -5.48 | -4.75 | -4.85 | -3.68 | -6.21 | -4.62 |
| Trifluoroacetonitrile | -1.53 | -0.53 | -1.20 | -0.64[#] | -2.10 | -2.24 |
| Methyl isocyanide | -4.84 | -3.74 | -4.15 | -3.01 | -5.46 | -3.41 |
| Methyl azide | -3.41 | -1.95 | -0.66 | -1.39 | -3.50 | -1.96 |
| Methyl cyanate | -8.69 | -7.27 | -7.46 | -6.29 | -8.91 | -6.29 |
| Methyl isothiocyanate | -4.45 | -2.35 | -2.82 | -2.27 | -5.74 | -4.22 |
| Cyclopentanone | -7.68 | -4.27 | -4.70 | -2.88 | -7.38 | -6.69 |
| Methyl acetate | -5.14 | -3.27 | -3.07 | -2.36[#] | -4.72 | -3.63 |
| Dimethyl sulfoxide | -12.03 | -17.27 | -15.54 | -8.47 | -13.82 | -9.19 |
| Dimethyl sufone | -11.26 | -17.75 | -15.76 | -7.83 | -13.36 | -9.94 |

[#] A considerable change in geometry compared to M06L. Do not show Xé X interaction.

## Conclusions

Clear evidence for intermolecular Xé X interaction (where X = C, N and O) between atoms of similar chemical environment in homogeneous dimers of organic molecules are obtained from MO, NBO and electron density analyses. The bonding is explained as resulting from the interaction between electron rich region of X atom in one monomer with electron deficient region of X atom in another monomer and also satisfying the condition that both X are from similar chemical environment. These X atoms are locally polarized as if one half is behaving electron rich compared to the other half. NBO analysis shows charge transfer between the two X atoms supporting the assumption that both X atoms act as both donor and acceptor. Binding energy of the dimers increases with increase in the dipole moment of the constituent monomers. Even in compounds with zero dipole moment such as acetylene and acetylene difluoride, induced dipoles in the dimer create bonding interaction. The EDA

analysis has shown that the binding energy ($E_{int}$), in most of the cases, is mainly electrostatic in nature. Further, the value of $E_{int}$ is divided into contribution from the total gain in electron density at the non-covalently interacting intermolecular bonds as well as a contribution from the monomer dipole moment. The dipole term contributes significantly to dimers of dipolar molecules where Xé X interaction from similar chemical environment exists. The Xé X interaction is characterized by a BCP in AIM analysis. The results are further validated by comparing the $E_{int}$ values with those calculated using different density functionals and G3MP2 methods and by predicting the G3MP2 $E_{int}$ values from ×ɟ and ε values. Crystal structures of several organic compounds with intermolecular Cé C inetraction between chemically similar carbon atoms are located in the literature. This suggests that these interactions can play a role in the crystal growth patterns as well as self assembly process of unsaturated organic molecules, which require further investigation.

## Acknowledgements

This research work is supported by the Council of Scientific and Industrial Research (CSIR), Govt. of India, through a project CSC0129. K.R. is thankful to CSIR, India, for providing a senior research fellowship.

## Notes and references

[a] *Inorganic and Theoretical Chemistry Section, CSTD, CSIR- National Institute for Interdisciplinary Science and Technology, , Trivandrum 695 019, India.. Tel: +91-471-2515472; E-mail: sureshch@gmail.com*

À Electronic Supplementary Information (ESI) available: [details of any supplementary information available should be included here]. See DOI: 10.1039/b000000x/

1. G. R. Desiraju and R. Parthasarathy, *J. Am. Chem. Soc.*, 1989, **111**, 8725-8726.
2. V. R. Pedireddi, D. S. Reddy, B. S. Goud, D. C. Craig, A. D. Rae and G. R. Desiraju, *J. Chem. Soc., Perkin Trans. 2*, 1994, 2353-2360.
3. J. P. M. Lommerse, A. J. Stone, R. Taylor and F. H. Allen, *J. Am. Chem. Soc.*, 1996, **118**, 3108-3116.
4. T. Clark, M. Hennemann, J. Murray and P. Politzer, *J Mol Model*, 2007, **13**, 291-296.
5. P. Metrangolo and G. Resnati, *Science*, 2008, **321**, 918-919.
6. P. Metrangolo, G. Resnati, T. Pilati and S. Biella, *Halogen Bonding in Crystal Engineering*, Springer Berlin Heidelberg, 2008.
7. A. C. Legon, *Phys. Chem. Chem. Phys.*, 2010, **12**, 7736-7747.
8. P. Politzer, J. S. Murray and T. Clark, *Phys. Chem. Chem. Phys.*, 2013, **15**, 11178-11189.
9. Y. Nagao, T. Hirata, S. Goto, S. Sano, A. Kakehi, K. Iizuka and M. Shiro, *J. Am. Chem. Soc.*, 1998, **120**, 3104-3110.
10. M. Iwaoka, S. Takemoto and S. Tomoda, *J. Am. Chem. Soc.*, 2002, **124**, 10613-10620.
11. D. B. Werz, R. Gleiter and F. Rominger, *J. Am. Chem. Soc.*, 2002, **124**, 10638-10639.
12. R. Gleiter, D. B. Werz and B. J. Rausch, *Chem. Eur. J.*, 2003, **9**, 2676-2683.
13. C. Bleiholder, D. B. Werz, H. Köppel and R. Gleiter, *J. Am. Chem. Soc.*, 2006, **128**, 2666-2674.
14. W. Wang, B. Ji and Y. Zhang, *J. Phys. Chem. A*, 2009, **113**, 8132-8135.
15. M. Solimannejad, M. Gharabaghi and S. Scheiner, *J. Chem. Phys.*, 2011, **134**, 024312.
16. S. Zahn, R. Frank, E. Hey-Hawkins and B. Kirchner, *Chem. Eur. J.*, 2011, **17**, 6034-6038.
17. A. Bauzá, T. J. Mooibroek and A. Frontera, *Angew. Chem. Int. Ed.*, 2013, **52**, 12317-12321.
18. A. Bundhun, P. Ramasami, J. Murray and P. Politzer, *J Mol Model*, 2013, **19**, 2739-2746.
19. D. Mani and E. Arunan, *Phys. Chem. Chem. Phys.*, 2013, **15**, 14377-14383.
20. L. M. Azofra, M. M. Quesada-Moreno, I. Alkorta, J. R. Aviles-Moreno, J. J. Lopez-Gonzalez and J. Elguero, *New J. Chem.*, 2014, **38**, 529-538.
21. A. Bauzá, R. Ramis and A. Frontera, *Comput. Theor. Chem.*, 2014, **1038**, 67-70.
22. S. J. Grabowski, *Phys. Chem. Chem. Phys.*, 2014, **16**, 1824-1834.
23. Q. Li, X. Guo, X. Yang, W. Li, J. Cheng and H.-B. Li, *Phys. Chem. Chem. Phys.*, 2014, **16**, 11617-11625.
24. D. Mani and E. Arunan, *The Journal of Physical Chemistry A*, 2014, **118**, 10081-10089.
25. S. A. C. McDowell, *Chem. Phys. Lett.*, 2014, **598**, 1-4.
26. S. A. C. McDowell and J. A. Joseph, *Phys. Chem. Chem. Phys.*, 2014, **16**, 10854-10860.
27. S. P. Thomas, M. S. Pavan and T. N. Guru Row, *Chem. Commun.*, 2014, **50**, 49-51.
28. P. R. Varadwaj, A. Varadwaj and B.-Y. Jin, *Phys. Chem. Chem. Phys.*, 2014, **16**, 17238-17252.
29. J. S. Murray, L. Macaveiu and P. Politzer, *J. Comput. Sci.*, 2014, **5**, 590 - 596.
30. J. Murray, P. Lane, T. Clark and P. Politzer, *J Mol Model*, 2007, **13**, 1033-1038.
31. J. S. Murray, P. Lane and P. Politzer, *Int. J. Quantum Chem.*, 2007, **107**, 2286-2292.
32. J. Murray, P. Lane and P. Politzer, *J Mol Model*, 2009, **15**, 723-729.
33. K. Remya and C. H. Suresh, *J. Comput. Chem.*, 2014, **35**, 910-922.
34. T. N. G. Row and R. Parthasarathy, *J. Am. Chem. Soc.*, 1981, **103**, 477-479.
35. D. B. Werz, R. Gleiter and F. Rominger, *Journal of the American Chemical Society*, 2002, **124**, 10638-10639.
36. M. Bai, S. P. Thomas, R. Kottokkaran, S. K. Nayak, P. C. Ramamurthy and T. N. Guru Row, *Cryst. Growth Des.*, 2013, **14**, 459-466.
37. Y. Zhao and D. G. Truhlar, *J. Chem. Phys.*, 2006, **125**, 194101: 194101-194118.
38. K. Remya and C. H. Suresh, *J. Comput. Chem.*, 2013, **34**, 1341-1353.
39. M. J. Frisch, G. W. Trucks, H. B. Schlegel, G. E. Scuseria, M. A. Robb, J. R. Cheeseman, G. Scalmani, V. Barone, B. Mennucci, G. A. Petersson, H. Nakatsuji, M. Caricato, X. Li, H. P. Hratchian, A. F. Izmaylov, J. Bloino, G. Zheng, J. L. Sonnenberg, M. Hada, M. Ehara, K. Toyota, R. Fukuda, J. Hasegawa, M. Ishida, T. Nakajima, Y. Honda, O. Kitao, H. Nakai, T. Vreven, J. J. A. Montgomery, J. E. Peralta, F. Ogliaro, M. Bearpark, J. J. Heyd, E. Brothers, K. N. Kudin, V. N. Staroverov, T. Keith, R. Kobayashi, J. Normand, K.

Raghavachari, A. Rendell, J. C. Burant, S. S. Iyengar, J. Tomasi, M. Cossi, N. Rega, J. M. Millam, M. Klene, J. E. Knox, J. B. Cross, V. Bakken, C. Adamo, J. Jaramillo, R. Gomperts, R. E. Stratmann, O. Yazyev, A. J. Austin, R. Cammi, C. Pomelli, J. W. Ochterski, R. L. Martin, K. Morokuma, V. G. Zakrzewski, G. A. Voth, P. Salvador, J. J. Dannenberg, S. Dapprich, A. D. Daniels, O. Farkas, J. B. Foresman, J. V. Ortiz, J. Cioslowski and D. J. Fox *Gaussian 09, Revision D.01*; Gaussian, Inc.: Wallingford CT, 2010

40. S. F. Boys and F. Bernardi, *Mol. Phys.*, 1970, **19**, 553-566.
41. T. Yanai, D. Tew and N. Handy, *Chem. Phys. Lett.*, 2004, **393**, 51-57.
42. A. D. Becke, *J. Chem. Phys.*, 1993, **98**, 5648-5652.
43. F. A. Hamprecht, A. Cohen, D. J. Tozer and N. C. Handy, *J. Chem. Phys.*, 1998, **109**, 6264-6271.
44. S. Grimme, S. Ehrlich and L. Goerigk, *J. Comp. Chem.*, 2011, **32** 1456-1465.
45. L. A. Curtiss, P. C. Redfern, K. Raghavachari, V. Rassolov and J. A. Pople, *J. Chem. Phys.*, 1999, **110** 4703-4709.
46. R. F. W. Bader, *Atoms in Molecules: A Quantum Theory*, Clarendon Press, Oxford, 1990.
47. F. Biegler-König, J. Schönbohm, R. Derdau, D. Bayles and R. F. W. Bader *AIM2000 Version 1* Germany, 2000
48. F. Biegler-König, J. Schönbohm and D. Bayles, *J. Comput. Chem.*, 2001, **22**, 545-559.
49. F. Biegler-König and J. Schönbohm, *J. Comput. Chem.*, 2002, **23**, 1489-1494.
50. T. A. Keith *AIMAll (Version 14.04.17)*; TK Gristmill Software: Overland Park KS, USA, 2014
51. J. S. Murray and K. Sen, *Molecular Electrostatic Potentials: Concepts and Applications*, Elsevier Science, Amsterdam, The Netherlands, 1996.
52. P. Politzer and D. G. Truhlar, *Chemical Applications of Atomic and Molecular Electrostatic Potentials: Reactivity, Structure, Scattering: Energetics of Organic, Inorganic, and Biological Systems*, Springer, New York, 1981.
53. S. R. Gadre and R. N. Shirsat, *Elelectrostatics of Atoms and Molecules*, Universities Press, Hyderabad, India, 2000.
54. N. Mohan and C. H. Suresh, *J. Phys. Chem. A*, 2014, **118**, 1697-1705.
55. P. Politzer and J. Murray, *J Mol Model*, 2015, **21**, 1-11.
56. T. Ziegler and A. Rauk, *Inorg. Chem.*, 1979, **18**, 1558-1565.
57. T. Ziegler and A. Rauk, *Inorg. Chem.*, 1979, **18**, 1755-1759.
58. F. M. Bickelhaupt and E. J. Baerends, in *Rev. Comput. Chem.*, eds. K. B. Lipkowitz and E. D. B. Boyd, Wiley-VCH, New York, 2000, vol. 15, pp. 1-86.
59. C. Fonseca Guerra, J. G. Snijders, G. te Velde and E. J. Baerends, *Theor. Chem. Acc.*, 1998, **99**, 391-403.
60. G. te Velde, F. M. Bickelhaupt, E. J. Baerends, C. Fonseca Guerra, S. J. A. van Gisbergen, J. G. Snijders and T. Ziegler, *J. Comput. Chem.*, 2001, **22**, 931-967.
61. E. J. Baerends, T. Ziegler, J. Autschbach, D. Bashford, A. Bérces, F. M. Bickelhaupt, P. M. B. C. Bo, L. Cavallo, D. P. Chong, L. Deng, R. M. Dickson, D. E. Ellis, M. v. Faassen, L. Fan, T. H. Fischer, C. F. Guerra, A. Ghysels, A. Giammona, S. J. A. v. Gisbergen, A. W. Götz, J. A. Groeneveld, O. V. Gritsenko, M. Grüning, S. Gusarov, F. E. Harris, P. v. d. Hoek, C. R. Jacob, H. Jacobsen, L. Jensen, J. W. Kaminski, G. v. Kessel, F. Kootstra, A. Kovalenko, M. V. Krykunov, E. v. Lenthe, D. A. McCormack, A. Michalak, M. Mitoraj, J. Neugebauer, V. P. Nicu, L. Noodleman, V. P. Osinga, S. Patchkovskii, P. H. T. Philipsen, D. Post, C. C. Pye, W. Ravenek, J. I. Rodríguez, P. Ros, P. R. T. Schipper, G. Schreckenbach, J. S. Seldenthuis, M. Seth, J. G. Snijders, M. Solà, M. Swart, D. Swerhone, G. t. Velde, P. Vernooijs, L. Versluis, L. Visscher, O. Visser, F. Wang, T. A. Wesolowski, E. M. v. Wezenbeek, G. Wiesenekker, S. K. Wolff, T. K. Woo and A. L. Yakovlev *ADF2010, SCM*; Theoretical Chemistry, Vrije Universiteit: Amsterdam, The Netherlands, 2010
62. K. Kitaura and K. Morokuma, *Int. J. Quantum Chem.*, 1976, **10**, 325-340.
63. F. Allen, *Acta Crystallogr., Sect. B*, 2002, **58**, 380-388.
64. F. Weinhold and C. R. Landis, *Valency and Bonding A Natural Bond Orbital Donor-Acceptor Perspective*, Cambridge University Press, UK, 2005.
65. S. J. Grabowski, *J. Phys. Chem. A*, 2001, **105**, 10739-10746.
66. O. Knop, K. N. Rankin and R. J. Boyd, *J. Phys. Chem. A*, 2002, **107**, 272-284.
67. R. Parthasarathi, V. Subramanian and N. Sathyamurthy, *J. Phys. Chem. A*, 2006, **110**, 3349-3351.
68. P. L. A. Popelier, *J. Phys. Chem. A*, 1998, **102**, 1873-1878.
69. U. Koch and P. L. A. Popelier, *J. Phys. Chem.*, 1995, **99**, 9747-9754.
70. A. S. Mahadevi, Y. I. Neela and G. N. Sastry, *Phys. Chem. Chem. Phys.*, 2011, **13**, 15211-15220.
71. A. Shahi and E. Arunan, *Phys. Chem. Chem. Phys.*, 2014, **16**, 22935-22952.
72. P. Politzer, J. S. Murray and T. Clark, *J. Mol. Model.*, 2015, **21**.
73. D. Sutor, *Acta Crystallogr.*, 1958, **11**, 453-458.
74. V. Enkelmann, *Chem. Mater.*, 1994, **6**, 1337-1340.
75. B. B. Frank, P. R. Laporta, B. Breiten, M. C. Kuzyk, P. D. Jarowski, W. B. Schweizer, P. Seiler, I. Biaggio, C. Boudon, J.-P. Gisselbrecht and F. Diederich, *Eur. J. Org. Chem.*, 2011, **2011**, 4307-4317.
76. T. Luu, E. Elliott, A. D. Slepkov, S. Eisler, R. McDonald, F. A. Hegmann and R. R. Tykwinski, *Org. Lett.*, 2004, **7**, 51-54.
77. R. R. Tykwinski, J. Kendall and R. McDonald, *Synlett*, 2009, **2009**, 2068-2075.
78. W. Changsheng, A. S. Batsanov, M. R. Bryce, S. Martin, R. J. Nichols, S. J. Higgins, V. M. Garcia-Suarez and C. J. Lambert, *J.Am.Chem.Soc.*, 2009, **131**, 15647-15654.
79. W. A. Chalifoux, R. McDonald, M. J. Ferguson and R. R. Tykwinski, *Angew. Chem. Int. Ed.*, 2009, **48**, 7915-7919.
80. J. R. Lane, J. Contreras-García, J.-P. Piquemal, B. J. Miller and H. G. Kjaergaard, *J. Chem. Theory Comput.*, 2013, **9**, 3263-3266.
81. C. Foroutan-Nejad, S. Shahbazian and R. Marek, *Chem. Eur. J.*, 2014, **20**, 10140-10152.